J|A|C|S
COMMUNICATIONS

Published on Web 05/24/2003

Catalytic Activity of Supported Au Nanoparticles Deposited from Block Copolymer Micelles

Thomas F. Jaramillo, Sung-Hyeon Baeck, Beatriz Roldan Cuenya, and Eric W. McFarland*

Department of Chemical Engineering, University of California, Santa Barbara, California 93106-5080

Received December 18, 2002; E-mail: mcfar@engineering.ucsb.edu

Bulk gold is considered catalytically inactive; however, isolated gold nanoparticles (<10 nm) have demonstrated high catalytic activity for both oxidation and reduction reactions.[1−8] The synthesis of nanoparticulate gold films on various supports has been accomplished by numerous techniques, including precipitation, physical vapor deposition (PVD), chemical vapor deposition (CVD), and organic encapsulation.[4−16] The latter technique, using block copolymer micelles to encapsulate the Au precursors, is a particularly attractive method for synthesis of Au-nanoparticle catalysts for several reasons: (1) quasi-hexagonal ordering of the Au clusters giving rise to high dispersions, (2) control of the intercluster spacing (surface density) by changing the length of the block copolymer tail,[13] (3) control of the cluster size distribution by the concentration of Au in solution and/or by selection of the appropriate length block copolymer head,[13−15] and (4) practicality of the dip-coating method which can be applied to most substrates. In this Communication, we report the size-dependent electro-oxidation of carbon monoxide as the first example of catalytic activity from Au nanoparticles synthesized by micelle encapsulation.

For the synthesis, 25 mg of the diblock copolymer [polystyrene$_{81\,000}$-*block*-poly(2-vinylpyridine)$_{14\,200}$] (from Polymer Source) was solvated in 5 mL of toluene.[13−15] The polymers form spherical micelles in which the polar poly-2-vinylpyridine (PVP) heads constitute the center and the nonpolar polystyrene (PS) tails extend outward. After the solution was vigorously stirred for approximately 5 h, 8.2 mg of $HAuCl_4 \cdot 3H_2O$ was added to the solution within a drybox. The resulting solution was subsequently stirred for 48 h, allowing the $AuCl_4^-$ adequate time to diffuse into the core of the micelle and to complex with the pyridine groups of PVP.

The micelles containing the gold nanoparticle precursors were dip-coated onto indium tin oxide (ITO)-coated glass substrates (30 mm × 4 mm × 0.7 mm).[17] The ITO substrates were affixed to an automated linear translation stage mounted in an upright position. The substrates were lowered into the Au-micelle solution at a speed of 100 μm/s until approximately 1.5 cm was immersed, at which time the motion was stopped for 5 s. The samples were then withdrawn at 100 μm/s. This dip-coating procedure deposited a monolayer of Au^{3+} nanoparticle-laden micelles on the surface. The N_2-dried samples were exposed to an oxygen plasma (110 W, 10 min, 300 mTorr) as the final processing step. The plasma serves two purposes: first, to remove the PS-PVP polymer and, second, to agglomerate the $[AuCl_4]^-$ complex into Au nanoparticles consisting of a Au^0 core and a Au_2O_3 shell.[13,14,16]

Figure 1 shows several micrographs of the Au nanoparticles prepared as described. AFM images of the ITO substrate before and after Au-nanoparticle dip-coating are shown in Figure 1a and b, respectively. Although the ITO is a rough substrate, gold nanoparticles were distinguishable. To avoid the AFM tip size limitations in determining the particle size, we coated the Au micelle solution onto carbon-coated copper TEM grids and imaged the samples before (c) and after (d) exposure to the oxygen plasma.

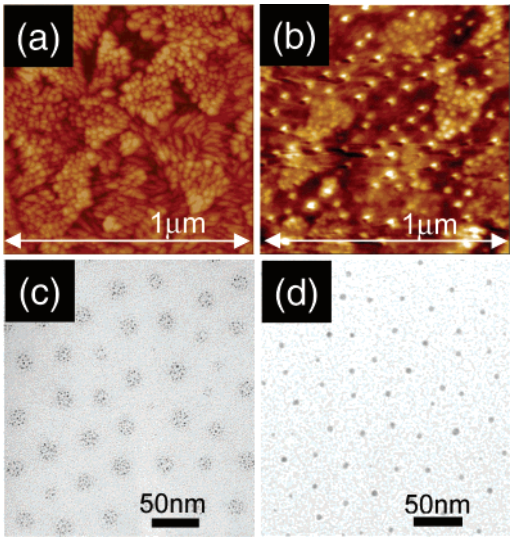

Figure 1. Micrographs of Au nanoparticles. (a) AFM of ITO-coated glass substrate; observed clusters are $In_2O_3-SnO_2$. (b) AFM of Au nanoparticles on ITO-coated glass (after O_2 plasma treatment). (c,d) TEM of Au nanoparticles on copper grid before (c) and after (d) plasma.

Figure 1c shows uniformly spaced (~50 nm) regions of distinct collections (~10−20 nm diameter) of relatively small electron-dense particles sparsely dispersed within each region. These particle collections are consistent with Au precipitate lining the PVP headgroups at the micelle core. The plasma treatment agglomerates the Au within each core region to single particles with an average size of 4.8 nm and standard deviation of 1.3 nm, Figure 1d.

X-ray (Al Kα radiation) photoelectron spectroscopy (XPS) was used to investigate the valence of the Au on the ITO films before and after O_2 plasma treatment, Figure 2. The emission of 4-f photoelectrons from Au is identified in four peaks of the XPS spectra, two of which are assigned to Au^0 (87.7 and 84.0 eV) and two to Au^{3+} (90.1 and 86.4 eV).[9,16,18] Before exposure to the oxygen plasma, most of the gold is observed as Au^{3+} (from the $[AuCl_4]^-$ complex), Figure 2a. After plasma treatment, the relative peak intensities are reversed, Figure 2b, with Au^0 electron intensity greater than the Au^{3+} intensity (from Au_2O_3).[16] The Au collected at the micelle core appears to be stabilized as Au^{3+} until the micelle is removed by the plasma, allowing the reduction to Au^0, which is facilitated by the hydrocarbon oxidation. Because the oxide component of the Au^0/Au_2O_3 nanoparticles may be necessary for catalytic activity, the particles were deliberately not fully reduced with a hydrogen plasma or other treatment. The dependency between catalytic activity and Au valence will be explored in future work. XPS was also used to verify the removal of the polymer by oxygen plasma treatment − as expected, after plasma processing, the C 1s peak decreased to levels typical of any material synthesized outside UHV (data not shown).

10.1021/ja029800v CCC: $25.00

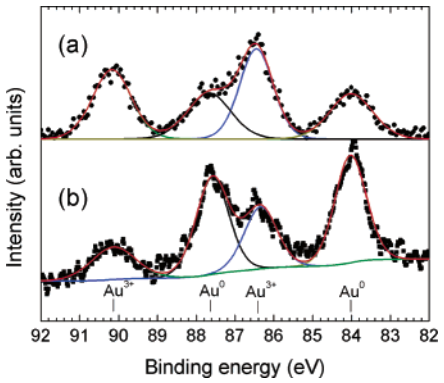

Figure 2. XPS of Au nanoparticles on ITO-coated glass before (a) and after (b) O_2 plasma treatment. Au^0 peaks are observed at binding energies of 87.7 eV (Au-$4f_{5/2}$) and 84.0 eV (Au-$4f_{7/2}$), while the oxide (Au^{3+}) is assigned to the peaks at 90.1 and 86.4 eV.[9,16,18] The relative area of the oxide peaks is larger than the zero-valence peaks in (a), but the opposite is true for (b), demonstrating that the O_2 plasma processing led to Au^0/Au_2O_3 nanoparticles that were mostly, but not entirely, in reduced form.

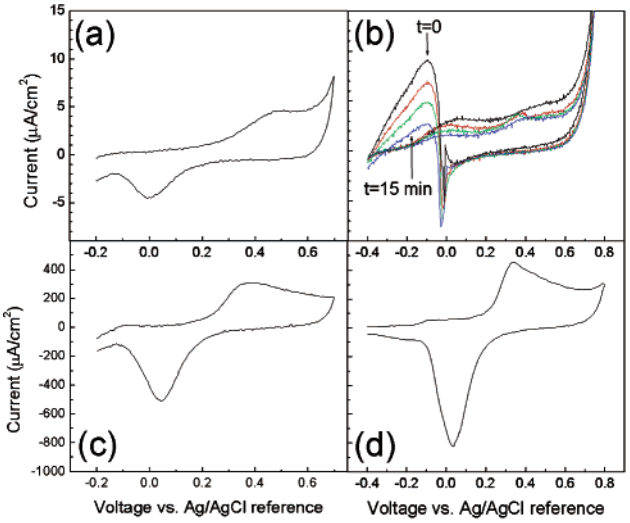

Figure 3. Electro-oxidation of carbon monoxide. Cyclic voltammograms were measured in 0.5 M KOH saturated with N_2 (a,c) and CO (b,d). (a) and (b) refer to nanoparticulate Au, while (c) and (d) pertain to bulk Au. The nanoparticulate Au catalyzes CO oxidation at −0.10 V (b); however, bulk gold shows no such evidence of electrocatalytic activity (d).

Electrocatalytic oxidation measurements of the oxygen plasma treated nanoclusters were obtained in 30 mL of 0.5 M KOH solution (ACS grade). The solution was first purged of oxygen by saturating with N_2 (99.998%, Praxair) for 30 min. Fifteen sequential cyclic voltammograms were immediately measured from the Au-nanoparticles on ITO in a three-electrode cell in the absence of O_2 at $t = 0$ (Pt mesh counter electrode, Ag/AgCl reference electrode). Consistent with previous work,[10] the adsorption and desorption of oxygen was observed at +0.50 and 0.00 V versus Ag/AgCl, respectively, Figure 3a. The presence of these peaks indicates that there is sufficient electrical contact between the ITO substrate and the Au-nanoparticles and minimal isolation of the Au by any residual polymer trapped under the clusters.

Cyclic voltammograms of the Au nanoparticles were repeated as the solution equilibrated in air to "activate" the surface for the electro-oxidation of CO.[6,8,10] The solution was then purged again with N_2 and subsequently saturated with carbon monoxide by bubbling with research grade CO (99.99%, Matheson Gas Products, Inc.). After saturation, the gas was stopped, and 25 cyclic voltammograms were measured over 15 min, several of which are shown in Figure 3b. The Au oxidation−reduction peaks showed small shifts as compared to the previous case (presumably due to the pH change), now at +0.40 and −0.02 V, respectively, and the primary CO electro-oxidation peak was observed at −0.10 V while scanning in the cathodic direction. With each successive cyclic voltammogram, the CO oxidation peak intensity decreases. This decrease can be attributed to the decrease in concentration of CO in solution, which results from two principal factors: (1) oxidation to CO_2 and (2) evolution of CO directly to the atmosphere. Results were reproduced upon resaturation of the solution with CO, and thus catalyst poisoning or delamination of Au was considered negligible in the short-term. Similar tests were conducted on bulk gold fabricated by evaporation (50 nm thick on ITO-coated glass), Figure 3c and d. Clearly, the adsorption and desorption of oxygen on Au is stronger in this thick Au film as compared to the Au nanoparticles. Nevertheless, the bulk Au film showed no activity for CO oxidation, whereas the Au nanoparticles were highly active.

For Au nanoparticles synthesized by block copolymer micelle encapsulation, these are the first observations of catalytic activity. The dip-coating method of synthesis produces a highly dispersed, quasi-regular array of Au nanoparticles (diameter 4.8 ± 1.3 nm) with tight control of particle size and can be applied to practically any substrate. Further investigation into CO oxidation as well as other electrochemical reactions, along with the dependence on substrate and particle size, is underway for gold nanoparticles fabricated by this versatile method.

Acknowledgment. The authors would like to thank the U.S. Air Force Office of Scientific Research for primary support of this work under AFOSR/DURINT grant #F49620-01-1-0459 and the U.S. Department of Energy for partial support under grant #DE-FC36-01G011092 and BES grant #DE-FG03-89ER14048. This work made use of MRL Central Facilities supported by the National Science Foundation under award DMR96-32716 and the UCSB Nanofabrication Facility. We would also like to thank Dr. Seong Heon Lee for his invaluable instructions on the nanoparticle synthesis and Ms. Anna Ivanovskaya and Mr. Jason Baxter for their technical assistance.

References

(1) Henry, C. *Appl. Surf. Sci.* **2000**, *164*, 252−259.
(2) Lopez, N.; Norskov, J. *J. Am. Chem. Soc.* **2002**, *124*, 11262−11263.
(3) Hostetler, M.; Zhong, C.-J. *J. Am. Chem. Soc.* **1998**, *120*, 9396−9397.
(4) Bond, G. C.; Thompson, D. T. *Catal. Reυ.* **1999**, *41*, 319−388.
(5) Haruta, M. *Catal. Today* **1997**, *36*, 153−166.
(6) Choudhary, T. V.; Goodman, D. W. *Top. Catal.* **2002**, *21*, 25−34.
(7) Hostetler, M.; Wingate, J. *Langmuir* **1998**, *14*, 17−30.
(8) Tateishi, N.; Nishimura, K. *J. Electroanal. Chem.* **1993**, *352*, 243−252.
(9) Brust, M.; Walker, M. *J. Chem. Soc., Chem. Commun.* **1994**, 801−802.
(10) Maye, M.; Lou, Y. *Langmuir* **2000**, *16*, 7520−7523.
(11) Lou, Y.; Maye, M. *Chem. Commun.* **2001**, 473−474.
(12) Song, Q.; Ai, X. *J. Nanopart. Res.* **2000**, *2*, 381−385.
(13) Spatz, J.; Mössmer, S. *Langmuir* **2000**, *16*, 407−415.
(14) Haupt, M.; Miller, S. *J. Appl. Phys.* **2002**, *91*, 6057−6059.
(15) Selvan, S. T.; Hayakawa, T. *J. Phys. Chem. B* **1999**, *103*, 7441−7448.
(16) Boyen, H. G.; Kästle, G. *Science* **2002**, *297*, 1533−1536.
(17) ITO-coated glass obtained from Delta Technologies, Inc. Polished float glass, SiO_2 passivated, $R_s = 4-8\ \Omega$, ~200 nm In_2O_3(90%)−SnO_2(10%).
(18) Juodkazis, K.; Juodkazyte, *J. Electrochem. Commun.* **2000**, *2*, 503−507.

JA029800V